

Giant optical Faraday rotation induced by a single-electron spin in a quantum dot: Applications to entangling remote spins via a single photon

C. Y. Hu,^{1,*} A. Young,¹ J. L. O'Brien,¹ W. J. Munro,^{2,3} and J. G. Rarity¹

¹*Department of Electrical and Electronic Engineering, University of Bristol, University Walk, Bristol BS8 1TR, United Kingdom*

²*Hewlett-Packard Laboratories, Filton Road, Stoke Gifford, Bristol BS34 8QZ, United Kingdom*

³*National Institute of Informatics, 2-1-2 Hitotsubashi, Chiyoda-ku, Tokyo 101-8430, Japan*

(Received 24 April 2008; published 13 August 2008)

We propose a quantum nondemolition method—a giant optical Faraday rotation near the resonant regime to measure a single-electron spin in a quantum dot inside a microcavity where a negatively charged exciton strongly couples to the cavity mode. Left-circularly and right-circularly polarized lights reflected from the cavity obtain different phase shifts due to cavity quantum electrodynamics and the optical spin selection rule. This yields giant and tunable Faraday rotation that can be easily detected experimentally. Based on this spin-detection technique, a deterministic photon-spin entangling gate and a scalable scheme to create remote spin entanglement via a single photon are proposed.

DOI: [10.1103/PhysRevB.78.085307](https://doi.org/10.1103/PhysRevB.78.085307)

PACS number(s): 78.67.Hc, 03.67.Mn, 42.50.Pq, 78.20.Ek

I. INTRODUCTION

Photons and semiconductor quantum-dot (QD) spins hold great promise in quantum information science, especially for quantum communications, quantum information processing, and quantum networks.^{1–6} Photons are ideal candidates to transmit quantum information with little decoherence whereas QD spins can be used to store and process quantum information due to the long electron-spin coherence time ($\sim\mu\text{s}$),⁷ which is limited by the spin-relaxation time ($\sim\text{ms}$).⁸ Therefore investigations of spin manipulation, spin detection, remote spin entanglement mediated by photons, and quantum state transfer between photons and spins are of great importance. Spin manipulation is well developed using pulsed magnetic-resonance techniques whereas single spin detection remains a challenging task. Quantum nondemolition (QND) measurement is highly desirable as it is a powerful resource for scalable quantum information processing. Recently, a method toward QND measurement⁹ of a single spin in a QD has been reported by Berezovsky *et al.*¹⁰ and Atatüre *et al.*¹¹ In order to minimize the disturbance to the electron spin, they use a probe beam off resonant with the QD transitions and the measured Faraday/Kerr rotation signals are rather weak.

In this paper, we propose a QND method—a giant optical Faraday rotation near the resonance regime to measure a single-electron spin in a single QD inside a microcavity. The different phase shifts for the left-circularly and right-circularly polarized lights reflected from the QD-cavity system yield giant Faraday rotation that can be easily detected experimentally. This giant Faraday rotation induced by a single-electron spin originates from the spin-dependent optical transitions of negatively charged exciton and the effect of cavity quantum electrodynamics (cavity-QED). Based on this spin-detection technique, we propose a deterministic photon-spin entangling gate and a scalable scheme to create remote spin entanglement via a single photon.

II. GIANT FARADAY ROTATION

We consider a singly charged QD, e.g., a self-assembled In(Ga)As QD or a GaAs interface QD inside an optical reso-

nant cavity. Figure 1(a) shows a micropillar cavity where the two GaAs/Al(Ga)As distributed Bragg reflectors (DBR) and the transverse index guiding provide the three-dimensional confinement of light. The QD is located in the center of the cavity to achieve maximal light-matter coupling. This kind of structure as well as microdisks and photonic crystal nanocavities have been used to make single-photon sources,^{12,13} and to study various cavity-QED effects.^{14–16}

If the QD is singly charged, i.e., an excess electron is injected into the QD, optical excitation can create a negatively charged exciton (X^-) that consists of two electrons bound to one hole.¹⁷ Due to Pauli's exclusion principle, X^- shows spin-dependent optical transitions [see Fig. 1(b)].¹⁸ If the excess electron lies in the spin state $|+\frac{1}{2}\rangle \equiv |\uparrow\rangle$, only the left-handed circularly polarized light (marked by $|L\rangle$ or L light) can be resonantly absorbed to create X^- in the state $|\uparrow\downarrow\uparrow\rangle$ with the two electron spins antiparallel. If the excess electron lies in the spin state $|-\frac{1}{2}\rangle \equiv |\downarrow\rangle$, only the right-handed circularly polarized light (marked by $|R\rangle$ or R light) can be resonantly absorbed and create a X^- in the state $|\uparrow\downarrow\downarrow\rangle$. Here $|\uparrow\rangle$ and $|\downarrow\rangle$ represent heavy-hole spin states $|\pm\frac{3}{2}\rangle$. The spin-quantization axis is along the QD growth direction, i.e., the normal direction of the cavity.

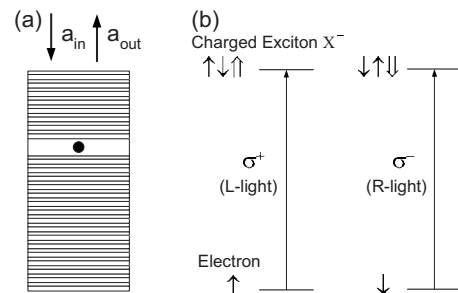


FIG. 1. (a) A charged QD inside a micropillar microcavity with circular cross section. The distributed Bragg mirrors and the index guiding provide three-dimensional confinement of light. (b) Spin selection rule for optical transitions of negatively charged exciton X^- in QD due to the Pauli's exclusion principle (see text).

However, the above spin selection rule only holds for an ideal QD that is symmetric in both the QD shape and the strain field distribution so that there is no spin-level mixing or splitting at zero magnetic field. A practical QD that is generally asymmetric can be made symmetric by applying an electric/magnetic field,¹⁹ thermal annealing,²⁰ or tuning the QD size.²¹ Due to this spin selection rule, the L and R lights encounter different phase shifts after reflection from the X^- -cavity system as discussed below.

The Heisenberg equations of motions for the cavity field operator \hat{a} and X^- dipole operator σ_- in the interaction picture, and the input-output relation are given by²²

$$\begin{cases} \frac{d\hat{a}}{dt} = - \left[i(\omega_c - \omega) + \frac{\kappa}{2} + \frac{\kappa_s}{2} \right] \hat{a} - g\sigma_- - \sqrt{\kappa}\hat{a}_{in} + \hat{H} \\ \frac{d\sigma_-}{dt} = - \left[i(\omega_{X^-} - \omega) + \frac{\gamma}{2} \right] \sigma_- - g\sigma_z\hat{a} + \hat{G} \\ \hat{a}_{out} = \hat{a}_{in} + \sqrt{\kappa}\hat{a} \end{cases}, \quad (1)$$

where ω , ω_c , and ω_{X^-} are the frequencies of external field (probe beam), cavity mode, and X^- transition, respectively. g is the coupling strength between X^- and the cavity mode. $\gamma/2$ is the X^- dipole decay rate, $\kappa/2$ is the cavity field decay rate into the input/output modes, and $\kappa_s/2$ into the leaky modes (side leakage). The material background absorption and losses in the back mirror can also be lumped in $\kappa_s/2$. \hat{H} and \hat{G} are the noise operators needed to conserve the commutation relations. \hat{a}_{in} and \hat{a}_{out} are the input and output field operators. Here we consider the single-sided cavity with the back mirror 100% reflective and the front mirror partially reflective. However, note that the inclusion of κ_s will lead to lower total reflectivities and the single-sided cavity hypothesis can model a real device.

If X^- stays in the ground state at most time, we can take $\langle \sigma_z \rangle \approx -1$ and $\sigma_z\hat{a} = -\hat{a}$. In the steady state, the reflection coefficient for the QD-cavity system can be obtained,

$$r(\omega) = 1 - \frac{\kappa \left[i(\omega_{X^-} - \omega) + \frac{\gamma}{2} \right]}{\left[i(\omega_{X^-} - \omega) + \frac{\gamma}{2} \right] \left[i(\omega_c - \omega) + \frac{\kappa}{2} + \frac{\kappa_s}{2} \right] + g^2}. \quad (2)$$

By taking $g=0$, we get the reflection coefficient for a cold cavity with QD uncoupled to the cavity,

$$r_0(\omega) = \frac{i(\omega_c - \omega) - \frac{\kappa}{2} + \frac{\kappa_s}{2}}{i(\omega_c - \omega) + \frac{\kappa}{2} + \frac{\kappa_s}{2}}. \quad (3)$$

If the main cavity decay rate outweighs the side leakage rate, Eq. (3) yields near-unity reflectance $|r_0(\omega)| \approx 1$ for the cold cavity in the whole frequency range. The side leakage (and unwanted absorption) can be made rather small by optimizing the etching process (or improving the sample growth).²³ In the following discussions, we neglect the side leakage first but come back to it later.

The complex reflection coefficients indicate that the reflected light feels a phase shift, which is a function of frequency detuning $(\omega - \omega_c)$ as presented in Fig. 2. For a cold

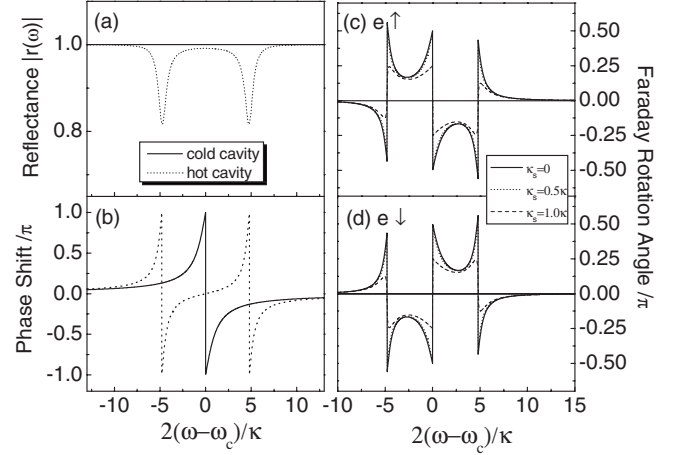


FIG. 2. Calculated (a) reflectance $|r(\omega)|$ and (b) phase shift vs frequency detuning from a cold cavity (solid curves) and a hot cavity (dotted curves). (c) and (d) show calculated Faraday rotation angle vs frequency detuning for different side leakage rates ($\kappa_s=0$ solid, $\kappa_s=0.5\kappa$ dot, and $\kappa_s=\kappa$ dash) when the electron is in the spin-up or spin-down states. $g/\kappa=2.4$ and $\gamma/\kappa=0.1$ are taken by considering the practical QD-cavity parameters (see text), and $\omega_{X^-} = \omega_c$ is assumed.

cavity, the phase shift is $\pm\pi$ at $\omega = \omega_c$ and decreases to zero with increasing frequency detuning [solid curve in Fig. 2(b)]. In the strong-coupling regime with $g \gg (\kappa, \gamma)$, the X^- state and cavity mode are mixed to form two new states, i.e., the dressed states, which lead to the vacuum-Rabi splitting. This state mixing results in a zero phase shift around $\omega = \omega_c$ and two phase structures corresponding to the two dressed states [dotted curve in Fig. 2(b)]. The strongly coupled X^- -cavity system is called a hot cavity hereafter. In the following we show that the different phase shifts induced by a cold cavity and a hot cavity can result in a giant Faraday rotation dependent on the state of the electron spin. We work near the resonant condition with $|\omega - \omega_c| \ll g$ so that the hot cavity has near-unity reflectance $|r_h(\omega)| \approx 1$ in the strong-coupling regime [see Fig. 2(a) and Eq. (2)]. As the cold cavity also shows unity reflectance, a linearly polarized probe beam remains linearly polarized after reflection.

As mentioned above, if the excess electron lies in the spin state $|\uparrow\rangle$, the L light feels a hot cavity and gets a phase shift of φ_h after reflection whereas the R light feels the cold cavity and gets a phase shift of φ_0 . As the linearly polarized probe beam can be regarded as the superposition of two circularly polarized components, i.e., $|R\rangle + |L\rangle$ (the factor $1/\sqrt{2}$ is neglected), the reflected light then becomes $e^{i\varphi_0}|R\rangle + e^{i\varphi_h}|L\rangle$. The polarization direction of the reflected light rotates an angle $\theta_F^\uparrow = \frac{\varphi_0 - \varphi_h}{2}$, which is the so-called Faraday rotation.

Conversely, if the excess electron lies in the spin state $|\downarrow\rangle$, the R light feels a hot cavity and gets a phase shift of φ_h after reflection whereas the L light feels the cold cavity and gets a phase shift of φ_0 . We thus get a Faraday rotation angle $\theta_F^\downarrow = \frac{\varphi_h - \varphi_0}{2} = -\theta_F^\uparrow$. The sign of Faraday rotation angle depends on the electron-spin state.

Figures 2(c) and 2(d) present the calculated Faraday rotation angle vs the frequency detuning. The side leakage can reduce the Faraday rotation angle; however, when $\kappa_s < \kappa$, the

Faraday rotation spectra is not very sensitive to the side leakage, and the rotation angles lie in the range between $-\pi/2$ and $\pi/2$, which are huge compared with the reported Faraday rotation in the off-resonance regime.⁹⁻¹¹ We call it giant optical Faraday rotation, which allows a single-shot measurement of a single-electron spin.

If the electron lies in a superposition spin state $|\psi\rangle = \alpha|\uparrow\rangle + \beta|\downarrow\rangle$, after reflection, the light and spin states become entangled,

$$(|R\rangle + |L\rangle) \otimes (\alpha|\uparrow\rangle + \beta|\downarrow\rangle) \rightarrow e^{i\varphi_0} \times \{ \alpha[|R\rangle + e^{i(\varphi_h - \varphi_0)}|L\rangle]|\uparrow\rangle + \beta[e^{i(\varphi_h - \varphi_0)}|R\rangle + |L\rangle]|\downarrow\rangle \}. \quad (4)$$

To realize an ideal quantum measurement, we set $\varphi_h - \varphi_0 = \pm \pi/2$ by adjusting the frequency detuning to $\omega - \omega_c \approx \pm \kappa/2$ [see Fig. 2(b)] so that the two polarization states of light are orthogonal to each other.²⁴ If we measure the light in the polarization state $|+45^\circ\rangle \equiv (|R\rangle + i|L\rangle)/\sqrt{2}$ [or $|-45^\circ\rangle \equiv (|R\rangle - i|L\rangle)/\sqrt{2}$], the electron spin collapses to the $|\uparrow\rangle$ (or $|\downarrow\rangle$) state. Although giant Faraday rotation occurs near the resonance regime rather than the off-resonance regime,⁹⁻¹¹ the real excitation or recombination of X^- induced by the probe beam is strongly suppressed as the light frequency deviates from the two dressed X^- -cavity modes due to the vacuum-Rabi splitting. This is also the reason why the hot cavity has near-unity reflectance near the central frequency in this regime. Within the spin-relaxation time (\sim ms),⁸ repeated measurements then yield the same results so this single-shot spin-detection method is a QND measurement.⁹ Based on the above spin QND measurement, a QND measurement of a single photon could also be implemented.²⁵

The observation of giant Faraday rotation relies on the realization of the strongly coupled QD-cavity system, which has been demonstrated recently in various microcavities and nanocavities.¹⁴⁻¹⁶ For micropillars with diameter around $1.5 \mu\text{m}$, the coupling strength $g = 80 \mu\text{eV}$ and the quality factor more than 4×10^4 (corresponding to $\kappa = 33 \mu\text{eV}$) have been reported,^{14,23} indicating $g/\kappa = 2.4$ is achievable for the In(Ga)As QD-cavity system. γ is about several μeV . Our calculations in Fig. 2 are based on these experimental values.

III. REMOTE SPIN ENTANGLEMENT VIA A SINGLE PHOTON

For single spin QND detection, the probe beam could be either weak coherent light or a train of single photons. When using a single photon as the probe beam, we can create entanglement between two remote spins in two spatially separated QD-cavity systems as shown in Fig. 3(a). Based on the discussions above, the X^- -cavity system can work as a photon-spin entangling gate if $g > (\kappa, \gamma)$ and $|\omega - \omega_c| \ll g$. We introduce the reflection operator

$$\begin{aligned} \hat{r}(\omega) &= |r_0(\omega)\rangle e^{i\varphi_0} (|R\rangle\langle R| \otimes |\uparrow\rangle\langle\uparrow| + |L\rangle\langle L| \otimes |\downarrow\rangle\langle\downarrow|) \\ &\quad + |r_h(\omega)\rangle e^{i\varphi_h} (|L\rangle\langle L| \otimes |\uparrow\rangle\langle\uparrow| + |R\rangle\langle R| \otimes |\downarrow\rangle\langle\downarrow|) \\ &= |r_0(\omega)\rangle e^{i\varphi_0} \hat{U}(\varphi), \end{aligned} \quad (5)$$

where $\hat{U}(\varphi)$ is the phase-shift operator defined as

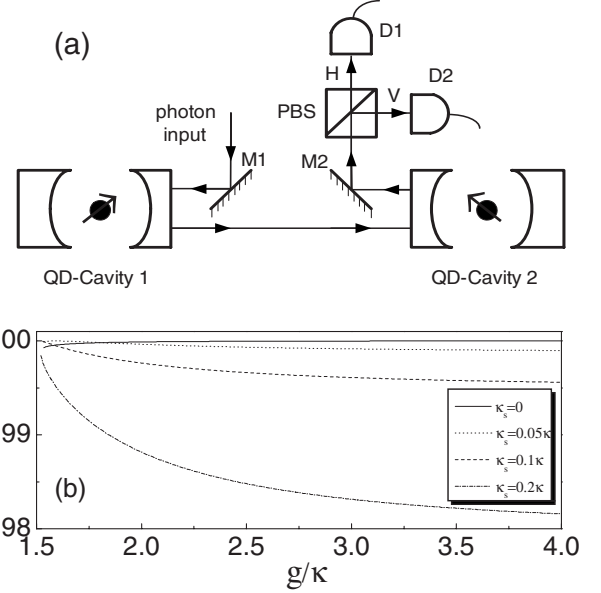


FIG. 3. (a) A proposed scheme to create entanglement between two remote spins via a single photon. M1 and M2 (reflection mirrors), polarized beam splitter (PBS) and D1 and D2 (detectors). (b) Entanglement fidelity vs the coupling strength for different side leakage rates ($\kappa_s = 0$ solid, $\kappa_s = 0.05\kappa$ dot, $\kappa_s = 0.1\kappa$ dash, and $\kappa_s = 0.2\kappa$ dash-dot). The curves are cut off for $g < 1.5\kappa$ as $\varphi_h(\omega) - \varphi_0(\omega) = \pm \pi/2$ is not achievable in this regime (Ref. 24).

$$\hat{U}(\varphi) = e^{i\varphi(L)\langle L|\otimes|\uparrow\rangle\langle\uparrow| + |R\rangle\langle R|\otimes|\downarrow\rangle\langle\downarrow|}, \quad (6)$$

where $\varphi = \varphi_h - \varphi_0$. The reflection operator can be simplified as the phase-shift operator for $|r_h(\omega)| \approx 1$ and $|r_0(\omega)| \approx 1$ [or for balanced reflectance $|r_h(\omega)| = |r_0(\omega)|$]. In the first QD-cavity system with the phase-shift operator $\hat{U}(\varphi_1)$, the excess electron is prepared in the spin state $|\psi_1\rangle = \alpha_1|\uparrow\rangle_1 + \beta_1|\downarrow\rangle_1$; In the second QD-cavity system with the phase-shift operator $\hat{U}(\varphi_2)$, the excess electron is prepared in the spin state $|\psi_2\rangle = \alpha_2|\uparrow\rangle_2 + \beta_2|\downarrow\rangle_2$. Both QD-cavity systems are assumed to have the same $\omega_c = \omega_{X^-}$.

A linearly polarized single photon is reflected from the first cavity, then reflected from the second cavity, after which it is detected [see Fig. 3(a)]. The corresponding state transformation is

$$\begin{aligned} &(|R\rangle + |L\rangle) \otimes (\alpha_1|\uparrow\rangle_1 + \beta_1|\downarrow\rangle_1) \otimes (\alpha_2|\uparrow\rangle_2 + \beta_2|\downarrow\rangle_2) \\ &\rightarrow \alpha_1\alpha_2(|R\rangle + e^{i(\varphi_1 + \varphi_2)}|L\rangle)|\uparrow\rangle_1|\uparrow\rangle_2 + \beta_1\beta_2(e^{i(\varphi_1 + \varphi_2)}|R\rangle \\ &\quad + |L\rangle)|\downarrow\rangle_1|\downarrow\rangle_2 + \alpha_1\beta_2(e^{i\varphi_2}|R\rangle + e^{i\varphi_1}|L\rangle)|\uparrow\rangle_1|\downarrow\rangle_2 \\ &\quad + \beta_1\alpha_2(e^{i\varphi_1}|R\rangle + e^{i\varphi_2}|L\rangle)|\downarrow\rangle_1|\uparrow\rangle_2. \end{aligned} \quad (7)$$

When $\varphi_1 = \varphi_2 = \pi/2$ by adjusting the frequency detuning to $\omega - \omega_c \approx \kappa/2$ [see Fig. 2(b) and Ref. 24], the output state becomes

$$\begin{aligned} &(|R\rangle - |L\rangle)[\alpha_1\alpha_2|\uparrow\rangle_1|\uparrow\rangle_2 - \beta_1\beta_2|\downarrow\rangle_1|\downarrow\rangle_2] \\ &\quad + i(|R\rangle + |L\rangle)[\alpha_1\beta_2|\uparrow\rangle_1|\downarrow\rangle_2 + \alpha_2\beta_1|\downarrow\rangle_1|\uparrow\rangle_2]. \end{aligned} \quad (8)$$

The output photon states can be measured in orthogonal linear polarizations. On detecting the photon in the $|R\rangle - |L\rangle$

state (0° linear), we project Eq. (8) onto a two-spin entangled state

$$|\Phi_{12}\rangle = \alpha_1\alpha_2|\uparrow\rangle_1|\uparrow\rangle_2 - \beta_1\beta_2|\downarrow\rangle_1|\downarrow\rangle_2. \quad (9)$$

On detecting the photon in the $|R\rangle+|L\rangle$ state (90° linear), we project onto another two-spin entangled state

$$|\Psi_{12}\rangle = \alpha_1\beta_2|\uparrow\rangle_1|\downarrow\rangle_2 + \alpha_2\beta_1|\downarrow\rangle_1|\uparrow\rangle_2. \quad (10)$$

On setting the coefficients $\alpha_{1,2}$ and $\beta_{1,2}$ to $1/\sqrt{2}$, we get maximally entangled spin states.

This scheme can be extended to create remote multispin entangled states such as GHZ or cluster states. This would be to sequentially entangle pairs of the spins by repeating the above single-photon measurement scheme that leads to Eqs. (9) and (10), combined with controlled local spin rotations.

If the photon loss and the detection inefficiency are neglected, our entanglement scheme is deterministic. Other schemes based on quantum interference of emitted photons can generate remote atomic entanglement^{26,27} and could be extended to entangle distant spins.^{28,29} However these schemes suffer from low success probability.²⁷ Here we use a single-photon quantum bus to couple or entangle remote spins,³⁰ which is similar to the scheme proposed by Leuenberger *et al.*,³¹ and the probabilistic scheme using bright coherent light as proposed by van Loock *et al.* and Ladd *et al.*³²

The QD spin superposition state can be prepared, for example, by optical pumping and/or optical cooling³³ followed by single spin rotations using nanosecond microwave pulses or picosecond/femtosecond optical pulses.³⁴ We also assume the probe light (photon) pulse bandwidth is much smaller than the cavity broadening, i.e., $\Delta\omega \ll \kappa/2$, so the frequency detuning can be precisely set. Furthermore, the entangling gate described by Eq. (6) has a well-defined phase and the optical pulse shape remains unchanged on reflection. These photons could come from QD-based single-photon sources^{12,13} or from nanosecond laser pulses. Hence all preparation and measurement time scales are short compared to the spin coherence time ($\sim \mu\text{s}$).⁷

If the cavity side leakage is neglected, then our entanglement scheme can achieve unity success probability and near-unity fidelity in the strong-coupling regime [see Fig. 3(b)] as $|r_0(\omega)| \approx 1$ and $|r_h(\omega)| \approx 1$. However, this is a big challenge

for QD-micropillar cavities although significant progress has been made.²³ If the cavity side leakage κ_s is taken into account, the entanglement fidelity with respect to the entangled state described by Eq. (10) becomes

$$F = \frac{1}{\sqrt{1 + \frac{1}{4} \left[\frac{|r_0(\omega)|}{|r_h(\omega)|} - \frac{|r_h(\omega)|}{|r_0(\omega)|} \right]^2}}, \quad (11)$$

which is generally less than one. However, approximately when $\kappa_s < 0.05\kappa$, there is still a point where we can achieve unity fidelity as $|r_0(\omega)| = |r_h(\omega)|$ [see Fig. 3(b)]. The reflectance at this point is not unity so the gate success probability is reduced (the cavity reflectivity is 82% when $\kappa_s = 0.05\kappa$). $\kappa_s = 0.05\kappa$ could possibly be achieved by taking a pillar microcavity with the quality factor of $\sim 165\,000$ demonstrated in Ref. 23 and decreasing the reflection of the top mirror to reduce the quality factor to ~ 9000 , which is still in the strong-coupling regime.¹⁴ However, note that $|r_0(\omega)| \neq |r_h(\omega)|$ does not affect the entanglement fidelity with respect to the entangled state described by Eq. (9) and it remains unity even when $\kappa_s \neq 0$. By performing a single spin-flip operation, Eq. (9) can be transformed to Eq. (10).

IV. CONCLUSIONS

In conclusion, giant optical Faraday rotation induced by a single-electron spin in a QD is proposed as a result of cavity-QED. This enables us to do quantum nondemolition measurement of a single-electron spin and to build a deterministic photon-spin entangling gate. Based on it, a deterministic and scalable scheme to create remote spin entanglement is proposed. We can also extend this scheme to implement coherent quantum state transfer between photon and spin, and entangle independent photons.²⁵ We believe this work opens an avenue for solid-state quantum networks with single photons and single QD spins.

ACKNOWLEDGMENTS

C.Y.H. thanks M. Atatüre, S. Bose, and S. Popescu for helpful discussions. J.G.R. acknowledges support from the Royal Society. This work is partly funded by UK EPSRC-GB IRC in Quantum Information Processing, QAP (Contract No. EU IST015848), and MEXT from Japan.

*chengyong.hu@bristol.ac.uk

¹D. Loss and D. P. DiVincenzo, Phys. Rev. A **57**, 120 (1998).

²A. Imamoglu, D. D. Awschalom, G. Burkard, D. P. DiVincenzo, D. Loss, M. Sherwin, and A. Small, Phys. Rev. Lett. **83**, 4204 (1999).

³C. Piermarocchi, P. Chen, L. J. Sham, and D. G. Steel, Phys. Rev. Lett. **89**, 167402 (2002).

⁴T. Calarco, A. Datta, P. Fedichev, E. Pazy, and P. Zoller, Phys. Rev. A **68**, 012310 (2003).

⁵W. Yao, R.-B. Liu, and L. J. Sham, Phys. Rev. Lett. **95**, 030504 (2005).

⁶S. M. Clark, Kai-Mei C. Fu, T. D. Ladd, and Y. Yamamoto, Phys.

Rev. Lett. **99**, 040501 (2007).

⁷J. R. Petta, A. C. Johnson, J. M. Taylor, E. A. Laird, A. Yacoby, M. D. Lukin, C. M. Marcus, M. P. Hanson, and A. C. Gossard, Science **309**, 2180 (2005); A. Greilich, D. R. Yakovlev, A. Sha-baev, Al. L. Efros, I. A. Yugova, R. Oulton, V. Stavarache, D. Reuter, A. Wieck, and M. Bayer, *ibid.* **313**, 341 (2006).

⁸J. M. Elzerman, R. Hanson, L. H. Willems van Beveren, B. Witkamp, L. M. K. Vandersypen, and L. P. Kouwenhoven, Nature (London) **430**, 431 (2004); M. Kroutvar, Y. Ducommun, D. Heiss, M. Bichler, D. Schuh, G. Abstreiter, and J. J. Finley, *ibid.* **432**, 81 (2004).

- ⁹M. Sugita, S. Machida, and Y. Yamamoto, arXiv:quant-ph/0301064 (unpublished).
- ¹⁰J. Berezovsky, M. H. Mikkelsen, O. Gywat, N. G. Stoltz, L. A. Coldren, and D. D. Awschalom, *Science* **314**, 1916 (2006).
- ¹¹M. Atatüre, J. Dreiser, A. Badolato, and A. Imamoglu, *Nat. Phys.* **3**, 101 (2007).
- ¹²E. Moreau, I. Robert, J. M. Gérard, I. Abram, L. Manin, and V. Thierry-Mieg, *Appl. Phys. Lett.* **79**, 2865 (2001).
- ¹³M. Pelton, C. Santori, J. Vuckovic, B. Zhang, G. S. Solomon, J. Plant, and Y. Yamamoto, *Phys. Rev. Lett.* **89**, 233602 (2002).
- ¹⁴J. P. Reithmaier, G. Şek, A. Löffler, C. Hofmann, S. Kuhn, S. Reitzenstein, L. V. Keldysh, V. D. Kulakovskii, T. L. Reinecke, and A. Forchel, *Nature (London)* **432**, 197 (2004).
- ¹⁵T. Yoshie, A. Scherer, J. Hendrickson, G. Khitrova, H. M. Gibbs, G. Rupper, C. Ell, O. B. Shchekin, and D. G. Deppe, *Nature (London)* **432**, 200 (2004).
- ¹⁶E. Peter, P. Senellart, D. Martrou, A. Lemaître, J. Hours, J. M. Gérard, and J. Bloch, *Phys. Rev. Lett.* **95**, 067401 (2005).
- ¹⁷R. J. Warburton, C. S. Dürr, K. Karrai, J. P. Kotthaus, G. Medeiros-Ribeiro, and P. M. Petroff, *Phys. Rev. Lett.* **79**, 5282 (1997).
- ¹⁸C. Y. Hu, W. Ossau, D. R. Yakovlev, G. Landwehr, T. Wojtowicz, G. Karczewski, and J. Kossut, *Phys. Rev. B* **58**, R1766 (1998).
- ¹⁹R. M. Stevenson, R. J. Young, P. See, D. G. Gevaux, K. Cooper, P. Atkinson, I. Farrer, D. A. Ritchie, and A. J. Shields, *Phys. Rev. B* **73**, 033306 (2006).
- ²⁰W. Langbein, P. Borri, U. Woggon, V. Stavarache, D. Reuter, and A. D. Wieck, *Phys. Rev. B* **69**, 161301(R) (2004).
- ²¹R. Seguin, A. Schliwa, S. Rodt, K. Potschke, U. W. Pohl, and D. Bimberg, *Phys. Rev. Lett.* **95**, 257402 (2005).
- ²²D. F. Walls and G. J. Milburn, *Quantum Optics* (Springer-Verlag, Berlin, 1994).
- ²³S. Reitzenstein, C. Hofmann, A. Gorbunov, M. Strauß, S. H. Kwon, C. Schneider, A. Löffler, S. Höfling, M. Kamp, and A. Forchel, *Appl. Phys. Lett.* **90**, 251109 (2007).
- ²⁴Numerical calculations show $\varphi_h - \varphi_0 = \pm \pi/2$ is achievable when $g > 1.5\kappa$ if the side leakage is small.
- ²⁵C. Y. Hu, W. J. Munro, and J. G. Rarity, arXiv:0711.1431 (unpublished).
- ²⁶C. W. Chou, H. de Riedmatten, D. Felinto, S. V. Polyakov, S. J. van Enk, and H. J. Kimble, *Nature (London)* **438**, 828 (2005).
- ²⁷D. L. Moehring, P. Maunz, S. Olmschenk, K. C. Younge, D. N. Matsukevich, L. M. Duan, and C. Monroe, *Nature (London)* **449**, 68 (2007).
- ²⁸L. Childress, J. M. Taylor, A. S. Sørensen, and M. D. Lukin, *Phys. Rev. Lett.* **96**, 070504 (2006).
- ²⁹C. Simon, Y. M. Niquet, X. Caillet, J. Eymery, J. P. Poizat, and J. M. Gérard, *Phys. Rev. B* **75**, 081302(R) (2007).
- ³⁰T. P. Spiller, K. Nemoto, S. L. Braunstein, W. J. Munro, P. van Loock, and G. J. Milburn, *New J. Phys.* **8**, 30 (2006).
- ³¹M. N. Leuenberger, M. E. Flatté, and D. D. Awschalom, *Phys. Rev. Lett.* **94**, 107401 (2005).
- ³²P. van Loock, T. D. Ladd, K. Sanaka, F. Yamaguchi, K. Nemoto, W. J. Munro, and Y. Yamamoto, *Phys. Rev. Lett.* **96**, 240501 (2006); T. D. Ladd, P. van Loock, K. Nemoto, W. J. Munro, and Y. Yamamoto, *New J. Phys.* **8**, 184 (2006).
- ³³M. Atatüre, J. Dreiser, A. Badolato, A. Hogege, K. Karrai, and A. Imamoglu, *Science* **312**, 551 (2006); C. Emary, X. D. Xu, D. G. Steel, S. Saikin, and L. J. Sham, *Phys. Rev. Lett.* **98**, 047401 (2007).
- ³⁴J. A. Gupta, R. Knobel, N. Samarth, and D. D. Awschalom, *Science* **292**, 2458 (2001); P. C. Chen, C. Piermarocchi, L. J. Sham, D. Gammon, and D. G. Steel, *Phys. Rev. B* **69**, 075320 (2004); J. Berezovsky, M. H. Mikkelsen, N. G. Stoltz, L. A. Coldren, and D. D. Awschalom, *Science* **320**, 349 (2008).